tent with geophysical models, for example, B69 (*19*) and M94 (*20*). In comparing our laboratory-based lower mantle model with upper mantle model XPSR98 (*7*), we found a conductivity jump of two orders of magnitude at the 410-km discontinuity and a minor conductivity increase at 660-km depth where ringwoodite disproportionates to perovskite + magnesiowüstite.

According to the conductivity variation for a temperature variation of ±100°C, our results do not favor temperature increasing along the $(Mg_{0.88}Fe_{0.12})SiO_3$ perovskite 2000°C adiabat from 2300°C at 660-km depth (*23*) if the effects of Al_2O_3 on the conductivity of silicate perovskite are considered.

References and Notes

1. T. Irifune and A. E. Ringwood, in *High-Pressure Research in Mineral Physics*, vol. 39 of *Geophysical Monograph Series* (American Geophysical Union, Washington, DC, 1987), pp. 231–242; T. Irifune, *Nature* **370**, 131 (1994).
2. B. J. Wood and D. C. Rubie, *Science* **273**, 1522 (1996).
3. C. McCammon, *Nature* **387**, 694 (1997).
4. Negative activation volumes of 0.26 ± 0.03 cm^3 mol^{-1} for perovskite and 0.1 to 0.2 cm^3 mol^{-1} for perovskite-magnesiowüstite assemblages are consistent with the hopping conduction mechanism [(*24*); T. J. Shankland, J. Peyronneau, J.-P. Poirier, *Nature* **366**, 453 (1993); J. P. Poirier, A. Goddat, J. Peyronneau, *Philos. Trans. R. Soc. London Ser. A* **354**, 1361 (1996)].
5. After the sample was placed inside the octahedral pressure medium, the entire cell assembly was dried overnight at 70°C in a vacuum furnace.
6. Y. Xu, B. T. Poe, D. C. Rubie, in *The Review of High Pressure Science and Technology, Proceedings of JOINT AIRAPT-16 & HPCJ-38*, M. Nakahara, Ed. (Japan Society of High-Pressure Science and Technology, Kyoto, Japan, 1998), vol. 7, pp. 1526–1528.
7. Y. Xu, B. T. Poe, T. J. Shankland, D. C. Rubie, *Science* **280**, 1415 (1998) (Model XPSR98).
8. MgO rings are also in contact with the sample but have no effect on oxygen fugacity.
9. Conductivity $\sigma = 1/RQ$, where R is the resistance of sample and $Q = A/l$ is the geometric factor of the recovered sample ($A = \pi r^2$ is the area of the electrodes and l is the length of the sample). The maximum error of the sample's geometry is 20% according to microscopic examination.
10. The conductivities in results from duplicate experiments differ by less than 0.07 logarithmic units, where the difference is likely due to uncertainty in sample geometry (a maximum uncertainty in geometry of 20% gives a difference of 0.08 logarithmic units in conductivity).
11. Samples identical to those used for conductivity measurements were synthesized at the same conditions and examined with the Mössbauer milliprobe according to the procedure described previously [C. A. McCammon, M. Hutchison, J. Harris, *Science* **278**, 434 (1997)]. Mössbauer spectra of the samples show the presence of Fe^{2+} and Fe^{3+} and rapid electron transfer between Fe^{2+} and Fe^{3+}. The relative amount of Fe^{3+} can be determined from the relative areas corrected for differences in recoil-free fraction [C. A. McCammon, *Phys. Chem. Miner.* **25**, 292 (1998)].
12. T. Katsura, K. Sato, E. Ito, *Nature* **395**, 493 (1998) (Model KSI).
13. Katsura *et al.* (*12*) used an electrode with an area larger than the sample area, and the geometric factor of the Al_2O_3 container is about three times greater than that of the sample. According to previous results for Al_2O_3 [A. Duba, in *High-Pressure Researches in Geoscience*, W. Schreyer, Ed. (Schweizerbart'sche Verlagsbuchhandlung, Stuttgart, Germany, 1982), pp. 375–381], the conductivity of Al_2O_3 is only ~0.5 logarithmic units lower than that of the sample at 1600°C. This result implies that leakage current through the Al_2O_3 container could be equal to that through the sample at 1600°C. The activation energy should increase with temperature, because the activation energy of ~2.5 eV for Al_2O_3 is much higher than that of perovskite.
14. The quenched phase should maintain the proportion of Fe^{3+} at high temperature and cannot reach equilibrium at low temperature in a short time.
15. X. Li and R. Jeanloz, *J. Geophys. Res.* **95**, 5067 (1990).
16. A. E. Ringwood, *Composition and Petrology of the Earth's Mantle* (McGraw-Hill, New York, 1975).
17. The effect of pressure on conductivity is weak, and the activation volume should be small (*4*). The electrical conductivity of perovskite is sensitive to the amount of Fe^{3+} coupled with Al_2O_3, and so the effect of oxygen fugacity on Al-bearing perovskite is small. The effect of OH on the conductivity of silicate perovskite is still unknown. The effect of texture at high pressure is small if different minerals are homogeneously distributed and there is no partial melt present.
18. R. Boehler, *Annu. Rev. Earth Planet. Sci.* **24**, 15 (1996).
19. R. J. Banks, *Geophys. J. R. Astron. Soc.* **17**, 457 (1969) (model B69).
20. K. G. McLeod, *J. Geophys. Res.* **99**, 13577 (1994) (model M94).
21. K. Bahr, N. Olsen, T. J. Shankland, *Geophys. Res. Lett.* **20**, 2937 (1993) (models BOS93-1 and BOS93-2).
22. H. F. Petersons and S. Constable, *ibid.* **23**, 1461 (1996).
23. I. Jackson, *Geophys. J. Int.* **134**, 291 (1998).
24. J. Peyronneau and J. P. Poirier, *Nature* **342**, 537 (1989) (model PP89).

25. We thank T. J. Shankland, A. G. Duba, and D. C. Rubie for discussions and suggestions and H. Fischer, K. Klasinski, D. Krausse, H. Küfner, and H. Schulze for technical assistance. D. C. Rubie and S. Karato donated the San Carlos orthopyroxene.

22 July 1998; accepted 30 September 1998

Seismic Evidence for an Inner Core Transition Zone

Xiaodong Song and Don V. Helmberger

Seismic waves that traverse Earth's inner core along north-south paths produce unusually broad pulse shapes at long periods (compared with waves along east-west paths) and reflections from below the inner core boundary at short periods. The observations provide compelling evidence for a seismic velocity discontinuity along north-south paths about 200 kilometers below the inner core boundary separating an isotropic upper inner core from an anisotropic lower inner core. The triplication associated with such a structure might be responsible for reported waveform complexity of short-period inner core arrivals along north-south paths and, if the depth of the boundary is laterally variable, their large travel-time variation.

Earth's core consists of a solid inner core with a radius of 1220 km surrounded by a liquid iron-rich outer core with a radius of 3480 km. The inner core was formed by the freezing of the liquid outer core as the Earth's interior loses its primordial heat (*1*). It is thought that the slow growth of the inner core provides a source of energy to drive the geodynamo in the fluid outer core, which generates the Earth's magnetic field (*2*). Sixty years after the inner core was discovered in 1936 (*3*), seismic observations revealed that it was rotating relative to the mantle at about 1° per year (*4*). The inner core rotation is driven by magnetic coupling between the electrically conductive inner core and the geomagnetic field (*5*). Subsequent estimates of the rotation vary by one order of magnitude, from 3° per year (*6*) to 0.2° to 0.3° per year (*7*), depending on the measurements of time-dependent signals and the models of inner core anisotropy used to infer the rotation.

The hypothesis that the inner core is anisotropic was first proposed in 1986 (*8*) and the presence of significant anisotropy in the inner core is now well established (*9*). On average, the wave velocity is about 3% faster along north-south (NS) ray paths through the inner core than along east-west (EW) ray paths (*10*). However, the detailed structure of the inner core anisotropy appears to be complex with significant lateral and depth variations (*11–14*). Although anisotropy occurs throughout the bulk of the inner core (*15*), the upper part of the inner core has weak to negligible anisotropy (*11, 12*). In addition, seismograms produced by NS paths show inner core arrivals with smaller amplitudes (*16*) and more complex waveforms (*17*) at short periods. Here we present evidence for a transitional structure of a mostly isotropic upper inner core (UIC) surrounding an anisotropic lower inner core (LIC) (Fig. 1A). We show that the triplication (Fig. 1B) associated with the rapid increase of velocity at such a transition along NS paths provides a consistent explanation for the anomalously broad waveforms of PKP-DF phases (compared with PKP-BC or PKP-AB phases) on long-period and broadband seismograms (dominant period about 10 s) and reflections from within the inner core on short-period seismograms (period about 1 s). The PKP-DF (or simply DF) ray goes through the inner core, whereas the PKP-

X. D. Song, Lamont-Doherty Earth Observatory, Palisades, NY 10964, and Department of Earth and Environmental Sciences, Columbia University, New York, NY 10027, USA. D. V. Helmberger, Seismological Laboratory, California Institute of Technology, Pasadena, CA 91125, USA.

BC ray travels nearly the same path throughout the mantle and most of the outer core, but turns near the base of the outer core, and the PKP-AB ray turns in the mid-outer core. Establishment and characterization of such a transition is likely to be important for understanding the source of the inner core anisotropy under debate and the evolution and dynamics of the Earth's core in general.

The most compelling differences between observations along EW versus NS paths are shown in Fig. 2. The waveforms of the DF phases from the EW paths are similar to the corresponding BC waveforms with the exception of a slight broadening and less high frequency content in the DF waveforms due to inner core attenuation (*18*). The difference in time of the DF versus the BC arrivals is well predicted by the Preliminary Reference Earth Model PREM2 (*19*). In contrast, the DF phases from the NS paths arrive earlier than predicted by the reference model, as attributed to the inner core anisotropy, and have much broader waveforms than the corresponding BC and AB phases. Note the sharp contrast in DF waveforms and BC to DF differential times between the EW path from event 11 in the South Sandwich Islands (SSI) (Table 1) to station INCN in Korea and the NS paths from the same event to KDAK and COLA in Alaska and to INK in Canada.

Although the inner core attenuation may be anisotropic with higher attenuation along the NS direction (*20*), the anomalous broadening cannot be caused by the inner core attenuation alone based on the following arguments. First, compared with the amplitude ratios in the EW records, the amplitude ratios of these unusually broad DF arrivals to the BC arrivals in the broadband records are not small. Second, the broadband records of Vinnik *et al.* (*15*) from NS paths from SSI to eastern Siberia at larger distances (>170°) do not show such anomalous broadening in the DF waveforms; because DF waves spend more time in the inner core at larger distances, more broadening would be expected if the inner core attenuation were the cause (*21*). Nor can the anomalous broadening be explained by the earthquake sources or struc-

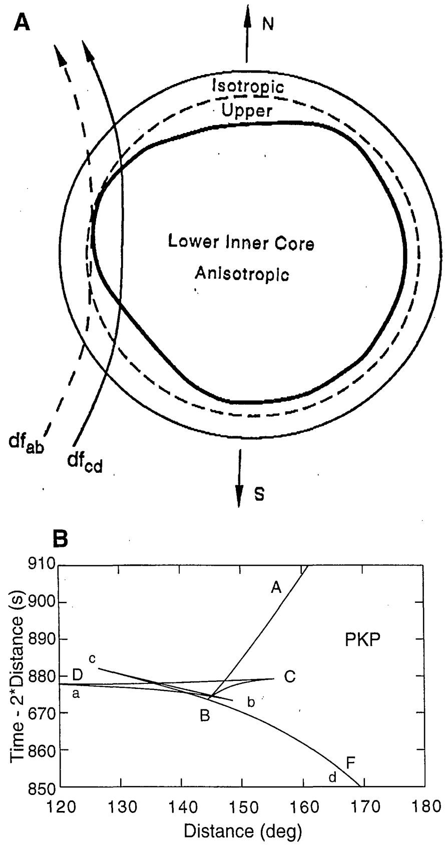

Fig. 1. (**A**) Schematic of isotropic UIC and anisotropic LIC structure. The UIC/LIC boundary (solid line) would give rise to multiple paths for seismic waves traveling nearly NS through the inner core at certain distances, producing distorted waveforms in long-period seismograms and multiple arrivals in short-period seismograms. The boundary is speculated to be irregular, which may explain recent reports of large scatter in inner core travel times (*14*). (**B**) Travel-time curves of seismic waves that go through the Earth's core (PKP) for an Earth model that includes a two-layered inner core with a velocity discontinuity at the boundary. Because of the discontinuity, waves that go through the inner core produce three branches (triplication) of arrivals, instead of one branch (DF): waves that turn in the upper inner core (DF_{ab}), waves that are reflected at the boundary (DF_{bc}), and waves that turn in the lower inner core (DF_{cd}).

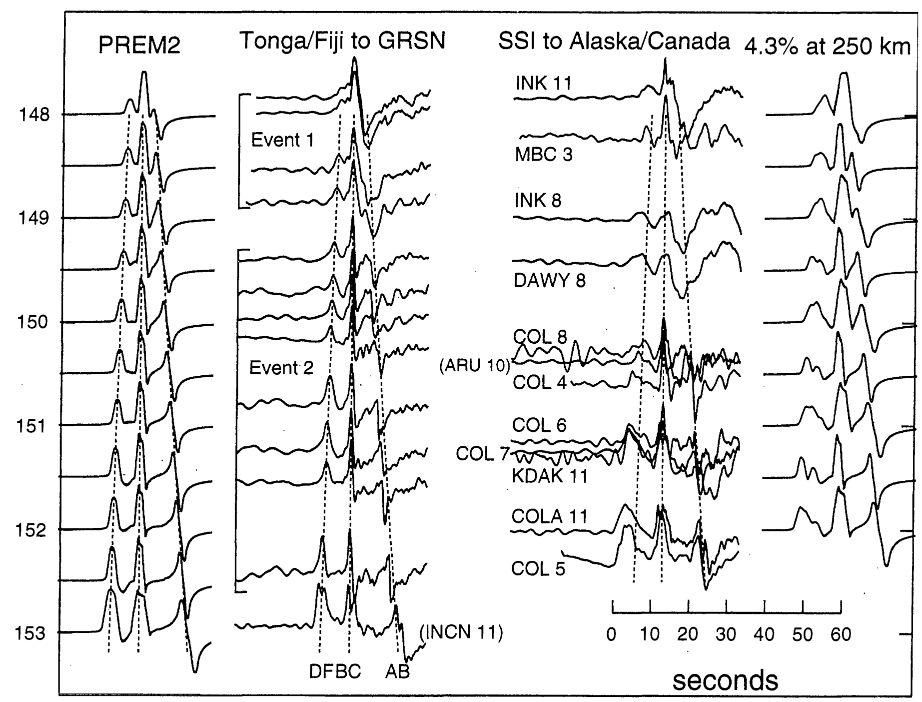

Fig. 2. (**Left to right**) Synthetics for PREM2, data from EW paths, data from NS paths, and synthetics for a model with a 4.3% P velocity jump at 250 km below the ICB. The PREM2 model (*19*), based on a modification of the Preliminary Reference Earth Model (*30*), was proposed to provide a better fit to the averages of PKP differential travel times and waveforms from EW paths. All the data are vertical displacement seismograms deconvolved from broadband digital records for events in the 1990s, or from long-period Worldwide Standardized Seismograph Network (WWSSN) records for events in the 1960s. Numerical labels indicate earthquake numbers in Table 1. The station codes are as follows: ARU, Arti, Russia; COL or COLA, College, Alaska; DAWY, Dawson, Yukon Territory, Canada; INCN, Inchon, Korea; INK, Inuvik, Northwest Territories, Canada; KDAK, Kodiak Island, Alaska; MBC, Mould Bay, Northwest Territories, Canada. All the NS paths are earthquakes in SSI to stations in Alaska and Canada (except that labeled ARU 10), which sample the inner core beneath Colombia and Venezuela. A long time window is used to show noise levels preceding the signals. The EW paths are from two events in the Tonga and Fiji Islands region to stations of the GRSN except the bottom trace (event 11 recorded at INCN). Dashed lines (left three columns) are relative travel times predicted for the PREM2 model at a source depth of 192 km. Synthetic seismograms (leftmost and rightmost two columns) are calculated by using generalized ray theory for a source depth at 192 km and 130 km, respectively, and an inner core attenuation factor $Q = 385$ (which corresponds to $t^* = 0.35$ s of PREM2 at 152°, where t^* is the travel time divided by Q and then integrated along the ray path through the inner core). The duration of the source time functions used for the synthetics of the leftmost column is 3 s (except the bottom trace, which has a 5-s duration). To simulate the different sources in the NS data, the durations of the source time functions used are 5 and 3 s, respectively, for the synthetics at whole degrees and those at half-degrees in the rightmost column. Note the broad DF waveforms from the NS paths are reasonably reproduced in these synthetics for the model with a velocity jump inside the inner core and the PREM2 synthetics agree well with the EW data.

ture in the mantle, which would affect BC and DF waves similarly because the two ray paths are nearly the same throughout the mantle. The observed phenomenon is also apparent in the records from SSI events to stations (DAWY, INK, and MBC) in Canada and in the record from an event in Drake Passage (between the southern tip of South America and Antarctica, to the west of SSI) to station ARU in Russia, so that it cannot be caused by local mantle structure such as a subduction slab beneath Alaska (*7*). The simplest explanation to the observed phenomenon is a triplication produced by a sudden increase in velocity along NS paths due to a change in the inner core anisotropy.

We computed synthetic seismograms for different models to match the observed broad DF waveforms (Fig. 2). The approach of waveform modeling has been a standard practice in seismology for a couple of decades (*22*) and it is particularly useful for identifying triplications. Synthetics generated for our smooth reference model, PREM2, fit the waveforms of the EW paths rather well. The model with a P velocity jump of 4.3% at 250 km below the inner core boundary (ICB) reproduces the broad DF waveforms of the NS paths reasonably well. Further tests show that models with a 3.5% jump at 200 km below the ICB and a 5% jump at 300 km below the ICB match the waveforms nearly as well. The broad DF waveforms in these synthetics are the results of overlapping energy of the waves that are refracted in the LIC (DF_{cd} branch in Fig. 1) and the waves that are refracted at the bottom of the UIC (DF_{ab} branch) or diffracted along the boundary (diffraction beyond the b cusp; Fig. 1B). To produce broad enough waveforms, the boundary needs to be relatively sharp (within 50 km in thickness). However, there is some model trade-off between the transition depth and the velocity jump.

Table 1. Earthquakes used in this study.

Event	Date	Location	Magnitude	Region
1	1995/10/06	20.00°S, 175.92°W, 198 km	5.8	Tonga Islands
2	1996/11/14	21.24°S, 176.62°W, 192 km	5.9	Fiji Islands
3	1966/10/11	60.50°S, 26.30°W, 36 km	5.8	SSI
4	1967/05/23	56.20°S, 27.29°W, 129 km	5.7	SSI
5	1967/06/17	58.30°S, 26.60°W, 140 km	6.1	SSI
6	1992/08/24	56.62°S, 26.55°W, 107 km	5.9	SSI
7	1992/11/21	56.67°S, 26.41°W, 20 km	5.9	SSI
8	1993/03/09	59.62°S, 25.709°W, 33 km	5.7	SSI
9	1993/05/22	55.98°S, 27.48°W, 113 km	5.3	SSI
10	1995/01/03	57.70°S, 65.88°W, 14 km	6.2	Drake Passage
11	1997/10/05	59.74°S, 29.20°W, 274 km	6.0	SSI

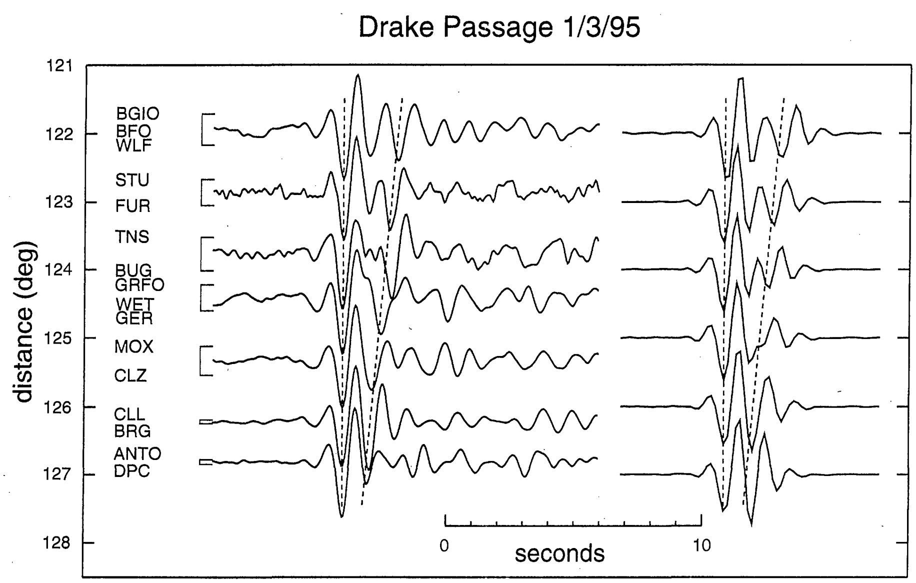

Fig. 3. (Left) Stacked short-period seismograms (vertical components) recorded at GRSN from an earthquake in Drake Passage (event 10), which sample the inner core beneath the central mid-Atlantic Ocean. Seismograms were obtained by convolving the original broadband displacement records with short-period WWSSN instruments, and the seismograms from neighboring stations (labeled) are stacked to enhance the secondary arrivals. Seismograms are aligned with PKiKP arrivals. Note clear secondary arrivals that lag further behind PKiKP at smaller distances. (Right) Synthetics calculated for a model with a 4% P jump at 95 km below the ICB and $t^* = 0.2$ s in the inner core. We used the t^* value that was obtained from modeling short-period waveforms of PKP waves sampling the upper 100 km of the inner core from the NS paths from SSI events to stations in the United States and Canada (*12*).

We have also observed direct evidence for a discontinuity within the inner core from short-period reflections in records from an earthquake in Drake Passage to the German Regional Seismic Network (GRSN) (Fig. 3). The record section provides dense coverage between 122° and 127°, where reflections from the ICB (PKiKP or CD branch in Fig. 1B) are often observed with a moderate-sized earthquake. When the records are aligned with the PKiKP arrivals, clear secondary arrivals, coming out of the tails of the PKiKP pulses, can be observed to move further away from PKiKP from 124° to 122° (Fig. 3, dashed line). At a distance of 122°, the secondary reflection arrives about 2.3 s after PKiKP with a ray parameter of about 14 s per radian smaller than that of PKiKP, which suggests that the reflector is about 95 km below the ICB. Synthetics for a model with a 4% jump at 95 km below the ICB (Fig. 3, right column) generally match the relative amplitudes and shapes of the later phases. Secondary inner core reflections such as these have been reported. Souriau and Souriau (*23*) observed near vertical reflections from 120 km below the ICB by stacking seismograms recorded at the Warramunga array in northern Australia from an earthquake in Loyalty Islands (curiously, an EW path) and suggested possible layering inside the inner core. Recently, Eakins *et al.* (*24*) also observed similar near vertical reflections at the ANZA broadband network in California from an earthquake 11 km southeast of the array.

For an inner core model with smooth velocity increase with depth, BC and DF waveforms are expected to have similar shapes. Generally, short-period DF phases are quite clear and strong for EW paths at distances 150° to 154° where BC phases are observable (*17*). But anomalous fast DF arrivals associated with NS paths have been well recognized to have small amplitudes and complicated waveforms at short periods (*16, 17, 25*), and separate phases are clearly observable within the DF time windows on some seismograms (*26*). The proposed strong inner core attenuation along NS paths (*20*) may explain the observed small amplitudes but not the waveform complexities. The transitional inner core structure we proposed here may offer an explanation. Such models with a jump would produce a triplication at short periods (Fig. 1B), which may appear as separate phases or cause complexity in the DF time window at short-period seismograms, much like the complexity found in upper mantle phases that result from upper mantle discontinuities. In defining the triplication, however, previous studies of the upper mantle discontinuities (*27*) suggest that long-period body waves as discussed above are more effective than short-period triplication data because short-period data are more prone to scattering.

The model we adopted with a sharp change of anisotropy at about 100 to 250 km depth of the inner core is not unique. For example, models with multiple boundaries may explain the data, as may models with the boundary depth varying laterally. Recent travel-time measurements for NS paths show considerable variation of over 2 s in BC − DF differential times from rays sampling different parts of the inner core (*14*). Large scatter in AB − DF is expected based on the large variation in the lowermost mantle (*28*). Scatter in BC − DF is more difficult to explain without variation in the inner core because the two rays are near each other when crossing the core-mantle boundary. The seismic data that sample the inner core reported here suggest variation of more than 100 km in the depth of the transition boundary over the sampling distance approximately equal to the radius of the inner core. Such large variation, as illustrated schematically in Fig. 1A, could produce the reported scatter of differential BC − DF travel times. This is rather speculative, however, and needs to be substantiated by more NS observations of short-period inner core reflections and modeling of long-period and broadband waveforms.

Naturally, the question of the physical or chemical cause of this inner core structure arises. Three structures of iron—face-centered cubic, hexagonal close-packed (hcp), and the recently discovered (*29*) β structures—are thought to be stable in the inner core. A phase transition from one structure of iron to another would be consistent with the sharp boundary that we have observed, but the depth of such a phase transition may not vary much laterally in the inner core where temperature variation is expected to be small. Alternatively, the observed boundary may mark the separation of randomly oriented anisotropic iron crystals in the upper part and those aligned preferentially NS in the lower part. If we assume hcp iron for the inner core, the velocity change across the boundary along the NS direction from the upper part of randomly oriented iron crystals to the lower part with iron crystals preferentially aligned, NS is expected to be two to three times the velocity change across the boundary along the EW direction, making the boundary more evident along NS paths as we reported here.

References and Notes

1. J. A. Jacobs, *Nature* **172**, 297 (1953).
2. S. I. Braginsky, *Dokl. Akad. Nauk. SSSR* **149**, 8 (1963).
3. I. Lehmann, *Bur. Cent. Seismol. Int. A* **14**, 3 (1936).
4. X. D. Song and P. G. Richards, *Nature* **382**, 221 (1996).
5. D. Gubbins, *J. Geophys. Res.* **86**, 11695 (1981); G. A. Glatzmaier and P. H. Roberts, *Phys. Earth Planet. Inter.* **91**, 63 (1995); J. M. Aurnou, D. Brito, P. L. Olson, *Geophys. Res. Lett.* **23**, 3401 (1996); W. J. Kuang and J. Bloxham, *Nature* **389**, 371 (1997).
6. W. J. Su, A. M. Dziewonski, R. Jeanloz, *Science* **274**, 1883 (1996).
7. K. C. Creager, *ibid.* **278**, 1284 (1997).
8. A. Morelli, A. M. Dziewonski, J. H. Woodhouse, *Geophys. Res. Lett.* **13**, 154 (1986); J. H. Woodhouse, D. Giardini, X.-D. Li, *ibid.*, p. 1549.
9. For a recent review, see X. D. Song [*Rev. Geophys.* **35**, 297 (1997)].
10. Unless otherwise noted, NS paths are used in this paper to mean those paths whose ray directions in the inner core are nearly parallel to (within 30°) Earth's spin axis, and EW paths are those whose ray directions in the inner core are nearly parallel (within 50°) to the equatorial plane.
11. P. M. Shearer, *J. Geophys. Res.* **99**, 19647 (1994).
12. X. D. Song and D. V. Helmberger, *ibid.* **100**, 9805 (1995).
13. W. J. Su and A. M. Dziewonski, *ibid.*, p. 9831.
14. S. Tanaka and H. Hamaguchi, *ibid.* **102**, 2925 (1997); K. C. Creager, paper presented at the 1996 Fall Meeting of the American Geophysical Union, San Francisco, CA, 15 December 1996.
15. L. Vinnik, B. Romanowicz, L. Breger, *Geophys. Res. Lett.* **21**, 1671 (1994); X. D. Song, *J. Geophys. Res.* **101**, 16089 (1996).
16. K. C. Creager, *Nature* **356**, 309 (1992).
17. X. D. Song and D. V. Helmberger, *Geophys. Res. Lett.* **20**, 2591 (1993).
18. D. J. Doornbos, *Geophys. J. R. Astron. Soc.* **38**, 397 (1974).
19. X. D. Song and D. V. Helmberger, *J. Geophys. Res.* **100**, 9817 (1995).
20. A. Souriau and B. Romanowicz, *Geophys. Res. Lett.* **23**, 1 (1996).
21. Here we assume that the attenuation anisotropy (with higher attenuation along NS paths) persists to great depth of the inner core, which also shows strong anisotropy in velocity (*15*). It is possible that the attenuation anisotropy changes with depth. Of the few models with strongest depth-dependent attenuation in the inner core [D. J. Doornbos, *Geophys. J. R. Astron. Soc.* **38**, 397, (1974); G. L. Choy and V. F. Cormier, *ibid.* **72**, 1 (1983)] we examined, we cannot account for the anomalous broadening at 151° and, at the same time, the lack of broadening at 173°.
22. D. V. Helmberger, *Earthquakes: Observation, Theory, and Interpretation*, International School of Physics "Enrico Fermi," Varenna, Italy, H. Kanamori, Ed. (North-Holland, New York, 1983), pp. 174–222; P. G. Richards, *The VELA Program: A Twenty-Five Year Review of Basic Research*, Defense Advanced Research Projects Agency, Arlington, VA, A. U. Kerr, Ed. (Executive Graphic Services, 1985), pp. 183–226.
23. A. Souriau and M. Souriau, *Geophys. J. Int.* **98**, 39 (1989).
24. J. Eakins, F. Vernon, G. Pavlis, R. Mellors, paper presented at the 1997 Fall Meeting of the American Geophysical Union, San Francisco, CA, 6 December 1997.
25. G. Masters, *Nature* **366**, 629 (1993).
26. One example is an event in SSI on 26 December 1984 recorded at COL in Alaska [Fig. 4 in (*17*)].
27. L. J. Burdick and D. V. Helmberger, *J. Geophys. Res.* **83**, 1699 (1978).
28. A large amount has been written about large lateral variation at the core-mantle boundary. For a recent review, see T. Lay, Q. Williams, E. J. Garnero, *Nature* **392**, 461 (1998).
29. S. K. Saxena *et al.*, *Science* **269**, 1703 (1995).
30. A. M. Dziewonski and D. L. Anderson, *Phys. Earth Planet. Inter.* **25**, 297 (1981).

31. Supported by the National Science Foundation. This work would not be possible without open access to the IRIS Data Management Center and the German GEOFONE Data Center. We thank X. M. Ding, J. Cassidy, S. Malone, and R. Lester for assistance in data collection. Comments from two anonymous reviewers greatly improved the manuscript.

13 May 1998; accepted 30 September 1998

Isotopic Evidence for the Cretaceous-Tertiary Impactor and Its Type

A. Shukolyukov and G. W. Lugmair

High-precision mass spectrometric analysis of chromium in sediment samples from the Cretaceous-Tertiary (K-T) boundary coincident with the extinction of numerous organisms on Earth confirms the cosmic origin of the K-T phenomenon. The isotopic composition of chromium in K-T boundary samples from Stevns Klint, Denmark, and Caravaca, Spain, is different from that of Earth and indicates its extraterrestrial source. The chromium isotopic signature is consistent with a carbonaceous chondrite–type impactor. The observed differences in the chromium isotopic composition among various meteorite classes can serve as a diagnostic tool for deciphering the nature of impactors that have collided with Earth during its history.

The discovery of high concentrations of Ir and other noble metals in K-T boundary sediments (*1*, *2*) led to the hypothesis that the worldwide enrichment of this and some other siderophile elements in the K-T boundary layer is due to an impact of asteroidal or cometary material 65 million years ago (Ma). This suggestion was based on the fact that the terrestrial crust is highly depleted in the noble metals as compared to the concentrations of noble metals in meteorites and because the terminal Cretaceous extinctions of terrestrial organisms occurred at the K-T boundary (*3*). However, the hypothesis on the cosmic origin of Ir and the concept of the extraterrestrial cause of the Cretaceous extinctions have not been unanimously accepted. Some researchers have argued that excess Ir and other phenomena observed at the K-T boundary can be explained by enhanced volca-

A. Shukolyukov, Scripps Institution of Oceanography, University of California, San Diego, La Jolla, CA 92093–0212, USA. G. W. Lugmair, Scripps Institution of Oceanography, University of California, San Diego, La Jolla, CA 92093–0212, USA, and Max-Planck-Institute for Chemistry, Cosmochemistry, Post Office Box 3060, 55020 Mainz, Germany.